Size Effects on the Optical Properties of Organic Nanoparticles

Hong-Bing Fu and Jian-Nian Yao*

Contribution from the Center for Molecular Science, Institute of Chemistry, CAS, Beijing 100080, People's Republic of China

Received July 17, 2000. Revised Manuscript Received October 31, 2000

Abstract: Nanoparticles of 1-phenyl-3-((dimethylamino)styryl)-5-((dimethylamino)phenyl)-2-pyrazoline (PDDP) ranging from tens to hundreds of nanometers were prepared by using the reprecipitation method. Their excitonic transitions responsible for absorption and emission, as compared with those of dilute solution, have been investigated as a function of nanoparticle size. We found that PDDP nanoparticles possess a special size dependence in their optical properties. We identified an extended charge-transfer (CT) state stemming from PDDP molecules closely stacking in nanoparticles and observed its shift to the high-energy side with decreasing nanoparticle size due to exciton confinement. At the same time, the molecular $\pi-\pi^*$ absorption of the nanoparticles was also blue-shifted, accompanied by an almost unchanging $n-\pi^*$ absorption as a result of the reduced overlap of the pyrazoline ring π orbital and decreased intermolecular interactions. Moreover, S1 and CT states were in equilibrium in the nanoparticles, and the probability of fluorescence from S1 increased with decreasing nanoparticle size.

Introduction

On the basis of the study of semiconductor and metal nanoparticles, many new physical phenomena, such as quantum confinement effects, finite size effects, etc., have been discovered, and many novel device concepts have been developed.[1−4] In recent years, the number of studies of organic nanoparticles has been increasing, but most such studies focus on polymers, such as polystyrene latex particles and its colloidal crystal.[5,6] However, the preparation of nanoparticles from general organic molecules has been paid little attention. Because of the diversity of organic molecules, there is a tendency to extend the research on nanoparticles from metals and semiconductors into the organic field, especially into general organic molecules. In the case of organic molecular crystals, their electronic and optical properties are fundamentally different from those of inorganic metals and semiconductors, due to weak intermolecular interaction forces of the van der Waals type.[7] To understand how these properties develop as a function of size is of fundamental and technological interest.

Nakanishi et al. prepared microcrystals of perylene and polydiacetylene by the simple reprecipitation method and found that polydiacetylene microcrystals were a new type of material for third-order nonlinear optics.[8−10] Pyrazolines have been widely used as optical brightening agents for textiles, paper, and fabrics because of their strong fluorescence[11,12] and as a hole-conveying medium in photoconductive materials[13,14] and electroluminescence (EL) devices.[15,16] Specifically, 2-pyrazolines containing electron donors and acceptors at the 1- and 3-positions have intrinsically large molecular hyperpolarizabilities, which suggests the photorefractivity of a two-dimensional array constructed with its nanoparticles in an applied optical field.[17] To some degree, 2-pyrazolines are considered to be an important organic heterocyclic "transition" material—i.e., a material which shares many properties with conventional semiconductors (with their delocalized electronic states) and insulator-like organic molecular crystals (with their large absorption oscillator strengths, polaron-assisted conduction, etc.).[7] In the work described in this paper, PDDP nanoparticles of different sizes have been prepared using the reprecipitation method, and their optical properties have been studied as a function of nanoparticle size. We have found that PDDP nanoparticles possess a special size dependence of absorption and emission, and the formation of the aggregates also influences the size dependence of PDDP nanoparticles in addition to previous opinions about the change of lattice state. The present optical size effects exhibited by PDDP nanoparticles may prove useful in optoelectronic device applications, such as optical modulators controlling the wavelength in organic photoconductors or electroluminescent materials, and in the study of the

* To whom correspondence should be addressed at Institute of Photographic Chemistry, Chinese Academy of Sciences, Beijing 100101, P.R. China. E-mail: jnyao@ipc.ac.cn.

(1) Halperin, W. P. *Rev. Mod. Phys.* **1986**, *58*, 533−606.
(2) Alivisatos, A. P. *Science* **1996**, *271*, 933.
(3) Peng, X. G.; Schlamp, M. C.; Kadavanich, A. V.; Alivisatos, A. P. *J. Am. Chem. Soc.* **1997**, *119*, 7019−7029.
(4) Yin, J. S.; Wang, Z. L. *Phys. Rev. Lett.* **1997**, *79*, 2570.
(5) Denkov, N. D.; Velev, O. D.; Kralchevsky, P. A.; Ivanov, I. B.; Yoshimura, H.; Nagayama, K. *Nature* **1993**, *361*, 26.
(6) Jiang, P.; Bertone, J. F.; Hwang, K. S.; Colvin, V. L. *Chem. Mater.* **1999**, *11*, 2132−2140.
(7) Silinsh, E. A. *Organic Molecular Crystals: Their Electronic States*; Springer-Verlag: Berlin, 1980.
(8) Kasai, H.; Kamatani, H.; Okada, S.; Oikawa, H.; Matsuda, H.; Nakanishi, H. *Jpn. J. Appl. Phys.* **1996**, *35* (Part 2, No. 2B), L221−L223.
(9) Kasai, H.; Kamatani, H.; Yoshikawa, Y.; Okada, S.; Oikawa, H.; Watanabe, A.; Itoh, O.; Nakanishi, H. *Chem. Lett.* **1997**, No. 9, 1181.
(10) Nakanishi, H.; Katagi, H. *Supramol. Sci.* **1998**, *5*, 289.
(11) Sandler, S. R.; Tsou, K. C. *J. Chem. Phys.* **1963**, *39*, 1062.
(12) Barbera, J.; Clays, K.; Gimenez, R.; Houbrechts, S.; Persoons, A.; Serrano, J. L. *J. Mater. Chem.* **1998**, *8*, 1725−1730.
(13) Borsenberger, P. M.; Schein, L. B. *J. Phys. Chem.* **1994**, *98*, 233.
(14) Melz, P. J.; Champ, R. B.; Chang, L. S.; Chiou, C.; Keller, G. S.; Liclican, L. C.; Neiman, R. R.; Schattuck, M. D.; Weiche, W. J. *Photo. Sci. Eng.* **1977**, *21*, 73.
(15) Gao, X. C.; Cao, H.; Zhang, L. Q.; Zhang, B. W.; Cao, Y.; Huang, C. H. *J. Mater. Chem.* **1999**, *9*, 1077−1080.
(16) Zhang, X. H.; Lai, W. Y.; Wu, S. K. *Chem. Phys. Lett.* **2000**, *320*, 77.
(17) Morley, J. O.; Docherty, V. J.; Pugh, D. *J. Mol. Electron.* **1989**, *5*, 117.

10.1021/ja0026298 CCC: $20.00
Published on Web 01/23/2001

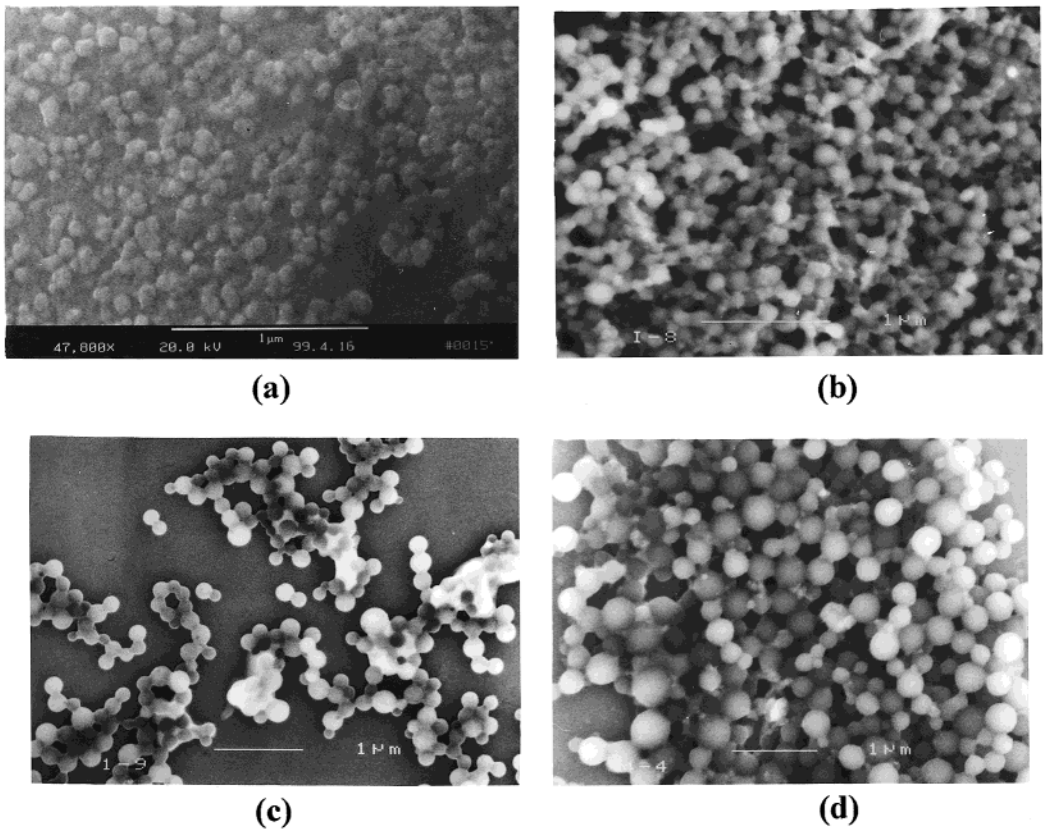

Figure 1. FESEM photographs of PDDP nanoparicles: (a) 50 nm, (b) 105 nm, (c) 190 nm, and (d) 310 nm.

fundamental process connecting both of these more conventional classes of materials, i.e., organic molecular crystals (OMCs).

Results

We prepared a series of PDDP nanoparticles from tens to hundreds nanometers, which were stable after two months. The nanoparticles' dispersions into water exhibited an off-white turbidity due to the light scattering of the nanoparticles. Moreover, the color deepened as the nanoparticle size increased. Some of their FESEM photographs are shown in Figure 1, in which the average nanoparticle sizes are 50, 105, 190, and 310 nm, respectively. These values agreed roughly with those determined by DLS, of which the polydispersity was measured to be less than 0.1. It can be seen from Figure 1 that the shape of the PDDP nanoparticles changed from perfectly spherical to amorphous with decreasing nanoparticle size. This implies that the crystallization of PDDP nanoparticles is gradually weakened with decreasing nanoparticle size. Measurements of the surface electric of the nanoparticles showed that they are negative charged, and the ξ-potential kept the same value of about -23 mV with different nanoparticle sizes.

Figure 2 displays the UV−visible absorption spectra of PDDP nanoparticles with different sizes dispersed in water. For comparison, the spectrum of dilute PDDP/ethanol solution (1.0×10^{-5} mol·L^{-1}), which has three clearly resolved peaks at 259, 314, and 378 nm, is also displayed as Figure 2m. Moreover, no spectral changes were observed when the concentration of PDDP/ethanol solution changed from 1.0×10^{-5} to 1.0×10^{-3} mol·L^{-1}. It has been reported that the UV band at 259 nm arises from the phenyl ring (labeled as P_{phenyl}) and the other two peaks at 314 and 378 nm are due to the pyrazoline ring n$-\pi^*$ ($P_{n-\pi^*}$) and $\pi-\pi^*$ ($P_{\pi-\pi^*}$) transitions, respectively.[18−20] The evolution

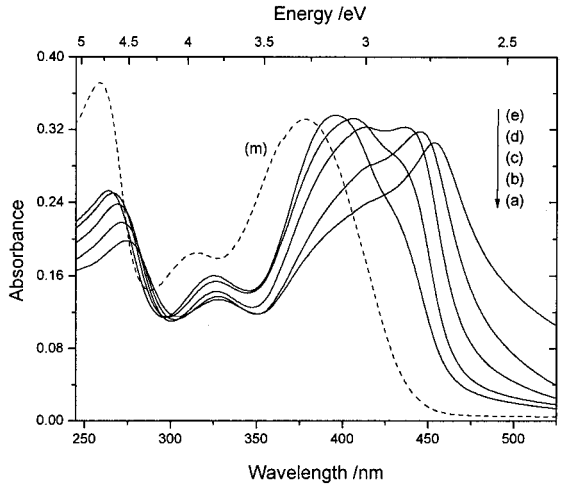

Figure 2. UV−visible absorption spectra of PDDP nanoparticles dispersions in water with different sizes: (a) 20 nm, (b) 50 nm, (c) 105 nm, (d) 190 nm, and (e) 310 nm. (m) The spectrum of the PDDP/ethanol solution (1.0×10^{-5} mol·L^{-1}).

of absorption features of PDDP nanoparticles is studied as a function of nanoparticle size upon going from Figure 2a to f. As the nanoparticle size increases from 20 to 310 nm, the P_{phenyl} and $P_{\pi-\pi^*}$ of PDDP nanoparticles are observed to shift to longer wavelength while the $P_{n-\pi^*}$ remains almost stable at the same position. At the same time, a new peak (P_{CT}) gradually appears in the region of 430−450 nm and also shifts to the lower energy side. It is obvious that these spectral changes are related to the nanoparticle size. To accurately determine the detailed behavior

(18) Mukai, M.; Miura, T.; Nanbu, M.; Shindo, T. Y. *Can. J. Chem.* **1979**, *57*, 360.

(19) Nurmukhametov, R. N.; Tishchenko, V. G. *Opt. Spectrosc.* **1967**, *23*, 83.

(20) Wilkinson, F.; Kelly, G. P.; Michael, C. *J. Photochem. Photobiol. A: Chem.* **1990**, *52*, 309−320.

Table 1. Results of Numerical Fit to the Absorption Spectra of PDDP Dilute Solution and Different Size Nanoparticles[a]

			absorption of pyrazoline ring					
			$[S_0(0)-S_2(0)]$		$[S_0(0)-S_1(n)]$		$[S_0(0)-CT(n)]$	
sample	nanoparticle size (nm)	absorption of phenyl (nm/eV)	position (nm/eV)	$F_{n-\pi^*}$ (%)	position (nm/eV)	$F_{\pi-\pi^*}$ (%)	position (nm/eV)	F_{CT} (%)
(m)	–	258	309	21.7	378	78.30	–	–
		4.81	4.01		3.28			
(a)	20	264	324	17.6	396	78.0	438	4.4
		4.70	3.83		3.13		2.83	
(b)	50	266	324	12.9	400	78.0	439	9.1
		4.66	3.83		3.10		2.83	
(c)	105	269	325	9.3	407	78.3	444	12.4
		4.61	3.82		3.05		2.79	
(d)	190	271	325	6.3	411	78.5	448	15.2
		4.58	3.82		3.02		2.77	
(e)	310	274	326	4.7	414	77.4	455	17.9
		4.53	3.80		3.00		2.73	

[a] Each spectrum in Figure 2 was fit to four Gaussian shapes. Because the absorption peak of the phenyl ring is not a Gaussian type, we directly read its wavelength from the software of the Shimadzu UV-1601 PC, while the data for the pyrazoline ring are obtained from the fitting results. $[S_0(0)-S_2(0)]$, $[S_0(0)-S_1(n)]$, and $[S_0(0)-CT(n)]$ correspond the transitions identified in the text and are expressed by peak position and peak area percentage for the whole pyrazoline ring absorption.

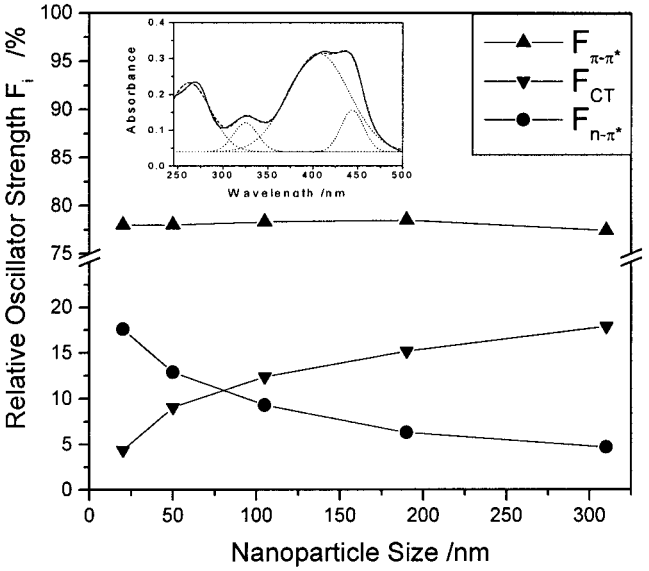

Figure 3. Relative oscillator strength F_i (proportional to the peak area and represented by area percentage of every peak for the whole pyrazoline absorption area) of absorption peak i ($P_{n-\pi^*}$, $P_{\pi-\pi^*}$, and P_{CT}) as a function of PDDP nanoparticle sizes. Inset: Sample numerical fit to the absorption spectrum with nanoparticle size 105 nm.

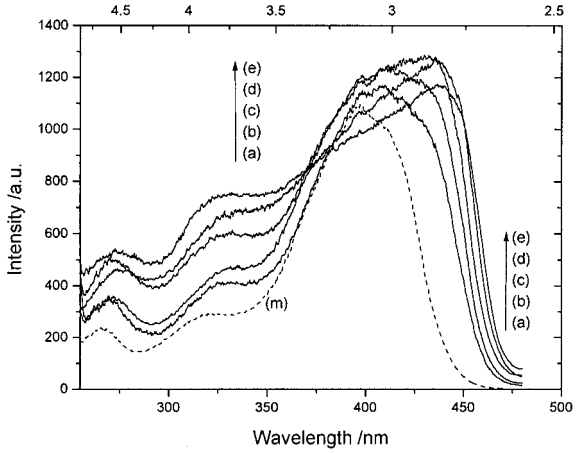

Figure 4. Fluorescence excitation spectra of PDDP nanoparticles dispersions in water with different sizes: (a) 20 nm, (b) 50 nm, (c) 105 nm, (d) 190 nm, and (e) 310 nm. (m) The spectrum of the PDDP/ethanol solution (1.0×10^{-5} mol·L^{-1}).

of absorption transitions on nanoparticle size, each spectrum was fit to four Gaussian peaks with the parameters provided in Table 1. The inset in Figure 3 is a sample fit to the spectrum of Figure 2c with the nanoparticle size of 105 nm. Because the peak P_{phenyl} is not a Gaussian type, in Table 1, its data were directly obtained from the software Schimadzu Uv-1601 PC, while the data of the other three peaks came from the results of fitting.

According to Table 1, as the size of PDDP nanoparticles increases from 20 to 310 nm, the P_{phenyl}, $P_{\pi-\pi^*}$, and the gradually appearing new peak P_{CT} are all shifted to lower energy, while the $P_{n-\pi^*}$ remains almost stable at 3.82 eV. Moreover, the energy decreases of $\Delta E(P_{phenyl}) = -0.17$ eV and $\Delta E(P_{\pi-\pi^*}) = -0.13$ eV are greater than that of $\Delta E(P_{CT}) = -0.10$ eV. Figure 3 shows the dependence of the area percentages (which are referred to as the relative oscillator strength, F_i) of the absorption peak i ($P_{n-\pi^*}$, $P_{\pi-\pi^*}$, and P_{CT}) for the whole pyrazoline ring absorption as a function of PDDP nanoparticle size. It can be seen from Figure 3 that the new peak in the region of 430−450 nm gradually increases from 4.4 to 17.9% with increasing nanoparticle size from 20 to 310 nm, while the $F_{n-\pi^*}$ gradually decreases from 17.6 to 4.7%. The most interesting observation is that the $F_{\pi-\pi^*}$ basically keeps the same value of about 78% with different nanoparticle sizes.

The fluorescence excitation spectra of PDDP nanoparticles with different sizes and PDDP monomer in the dilute ethanol solution displayed in Figure 4 show changes similar to those of the absorption spectra in Figure 2. As the nanoparticle size increases, the peak width becomes broader and its shape changes from symmetric to asymmetric, and at the same time, the peak also shifts to the longer wavelength region. Furthermore, the peak position where the fluorescence efficiency is the highest is consistent with the wavelength of the new absorption peak P_{CT} obtained from Figure 2. The low-energy tails of PDDP nanoparticles (defined as the energy at which the intensity is >5% of the peak intensity) extend to 2.66, 2.64, 2.62, 2.60, and 2.58 eV, corresponding to the crystal sizes 20, 50, 105, 190, and 310 nm, respectively. In contrast, the low-energy tail of the dilute PDDP solution only extends to 2.76 eV.

There are significant differences between the fluorescence emission spectra of the PDDP solution and PDDP nanoparticles in Figure 5. All these spectra are excited at 395 nm (3.14 eV). The PDDP solution emission spectrum (an asymmetric peak)

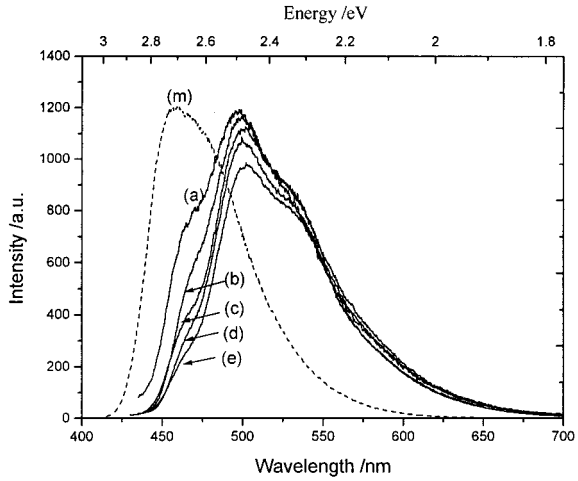

Figure 5. Fluorescence emission spectra of PDDP nanoparticles dispersions into water with different sizes: (a) 20 nm, (b) 50 nm, (c) 105 nm, (d) 190 nm, and (e) 310 nm. (m) The spectrum of the PDDP/ethanol solution (1.0×10^{-5} mol·L^{-1}).

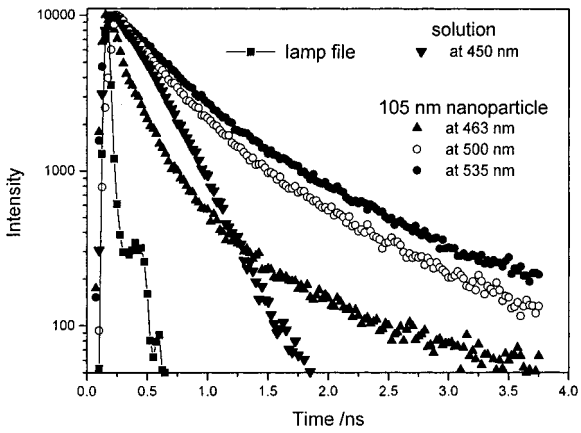

Figure 6. Fluorescence decay profiles of PDDP/ethanol solution (1.0×10^{-5} mol·L^{-1}) monitored at 450 nm (down triangle) and PDDP nanoparticle with size of 105 nm monitored at 463 (up triangle), 500 (open circle), and 535 nm (solid circle). The excitation wavelength is 320 nm.

has a maximum at about 450 nm (2.76 eV), and the low-energy tail extends to 2.17 eV. This is compared with that of PDDP nanoparticles with the emission peak centered at 500 nm (2.48 eV) and two additional features at 463 nm (2.68 eV) and 535 nm (2.32 eV). Moreover, the intensity of the shoulder at 2.68 eV gradually decreases with increasing nanoparticle size, but at the same time the remainder shows little change. No evident changes in the shape of the solution and the nanoparticles' emission spectra are observed as the pump energy changes from $E = 4.75$ to 2.76 eV.

To obtain further information on the nature of the excited state, we measured the fluorescence lifetimes of PDDP monomer in the dilute ethanol solution and different size PDDP nanoparticles in the aqueous dispersions with an excitation at 320 nm. Because no evident changes were observed for different size PDDP nanoparticles when other experimental conditions were fixed, the fluorescence decay profiles of 105 nm PDDP nanoparticles monitored at 463, 500, and 535 nm as a typical and PDDP monomer monitored at 450 nm were shown in Figure 6. The fluorescence decay data were best fitted with a double-exponential function by use of the nonlinear least-squares method with a deconvolution technique. The decay curve of the monomer monitored at 450 nm (down triangle in Figure 6) and those of 105 nm PDDP nanoparticles monitored at 500

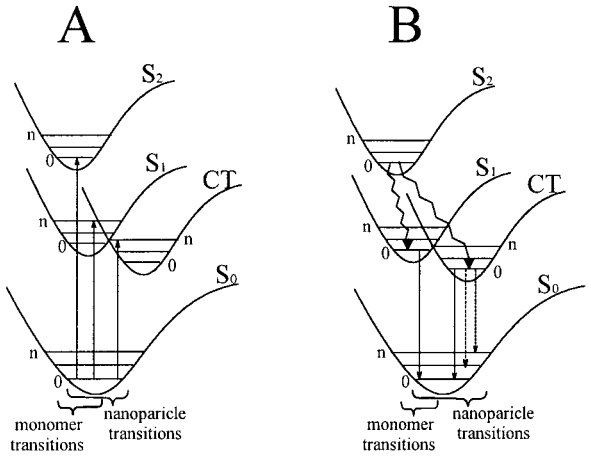

Figure 7. (A) Absorption and (B) emission transitions proposed for PDDP.

(open circle) and 535 nm (solid circle) are well described with only one τ with high accuracy. The fluorescence lifetime of the PDDP monomer was determined to be $\tau_m = 278 \pm 25$ ps. The fluorescence lifetimes of 105 nm PDDP nanoparticles monitored at 500 and 535 nm were determined to be nearly equal, $\tau_{500} = 601 \pm 80$ ps and $\tau_{535} = 693 \pm 80$ ps. However, the decay curve of the 105 nm PDDP nanoparticle monitored at 463 nm (up triangle in Figure 6) is well-resolved into two decay components with high accuracy, a short fluorescence lifetime $\tau'_{463} = 150 \pm 25$ ps (72%) and a long fluorescence lifetime $\tau''_{463} = 659 \pm 80$ ps (28%), respectively. It is interesting to note that the τ'_{463} is similar to τ_m and τ''_{463} is practically equal to the average of τ_{500} and τ_{535}.

Discussion

Absorption and Emission Transitions in the Dilute Solution and Nanoparticles. To interpret the data of Figures 1−6, we use an energy state diagram as shown in Figure 7. Here, Figure 7A corresponds to the absorption transitions, whereas Figure 7B corresponds to the emission transitions occurring after nuclear relaxation. The ground electronic state of PDDP is a spin-singlet and is labeled S_0. The high oscillator strength of the absorption features in Figure 2 is therefore a signature of spin-allowed singlet−singlet transitions. Since monomers are the dominant species in the dilute solution, further, the fluorescence emission spectrum does not significantly change with concentration, the solution emission in Figure 6 is assigned to direct monomer transitions from S_1 to S_0. The absorption transition from S_0 to high vibrational levels ($\nu_n = 0, ..., n$) of S_1 (labeled [$S_0(0)-S_1(n)$]) leads to the large Stokes shift of 0.52 eV; moreover, the [$S_0(0)-S_1(n)$] is $\pi-\pi^*$ type. The higher energy absorption n−π^* type (4.01 eV) than that of [$S_0(0)-S_1(n)$] (3.28 eV) leads us to assign it as being from S_0 to S_2, labeled [$S_0(0)-S_2(0)$].

For PDDP nanoparticles, the absorption transitions [$S_0(0)-S_1(n)$] and [$S_0(0)-S_2(0)$] are considered to be the contribution of individual molecules, i.e., Frenkle-like—the excitation is largely confined to the individual molecules. The distinctly different behavior of [$S_0(0)-S_1(n)$] and [$S_0(0)-S_2(0)$] as compared to the gradually appearing new peak P_{CT} leads us to assign these two groups of transitions to separate singlet manifolds. Returning to Figures 2 and 3, we observe that the absorption peak centered at about 430−450 nm is strongly affected by the nanoparticle sizes, becoming vanishingly small for crystals ≤20 nm. This is expected for an aggregate state arising from the $\pi-\pi$ orbital overlap of closely stacked PDDP

molecules in nanoparticles and is similar to the previous observations of absorption by aggregate states in other organic molecular crystals such as α-perylene,[21] tetracene,[22] and 3,4,9,-10-perylenetetracarboxylic dianhydride (PTCDA).[23] In addition, comparing Figure 2m with Figure 2a, although the concentration 1.0×10^{-5} mol·L^{-1} of the dilute PDDP/ethanol solution is greater than that of the 20 nm PDDP nanoparticle aqueous dispersion (prepared by injecting 40 μL of 1.0×10^{-3} mol·L^{-1} PDDP/ethanol solution into 10 mL of water at 0 °C), the former has no detectable peak in the region 430−450 nm but the latter does. From this, we infer that the peak centered at 438 nm in Figure 2a is associated only with aggregate formation and is non-Frenkel-like in nature; i.e., it is not associated with the lowest observed band S_1. Thus, we assign the gradually appearing absorption feature with increasing nanoparticle size to a charge-transfer (CT) exciton of the extended PDDP crystal structure. The lower energy of the 2.83−2.73 eV peak (labeled [$S_0(0)-CT(n)$]) as compared to that of the S_1 state is also consistent with this picture, where CT states are generally found at energies lower than the corresponding maxima of the monomer spectrum.[7,24]

Note that in Figure 5, without considering the shoulder at 2.68 eV, the shape of the nanoparticle emission is similar to that of the dilute solution, and its peak red shifts by 0.28 eV from the value for the dilute solution. The energy decrease of 0.28 eV is close to the energy difference between absorption transitions [$S_0(0)-S_1(n)$] and [$S_0(0)-CT(n)$]. Thus, the nanoparticle emission peak at 2.48 eV is from CT to the ground state (labeled [$CT(0)-S_0(0)$]). The additional emission feature at 2.32 eV results from vibrational characteristics (transitions as the dashed line arrows in Figure 7B), indicating some anharmonicity in the CT potential induced upon crystallization and subsequent exciton delocalization, or additional vibrational modes of PDDP in the solid state. Further, we assign the higher energy shoulder at 2.68 eV to be from S_1 to S_0 (labeled [$S_1(0)-S_0(0)$]). This is supported by the fluorescence lifetime measurements. In organic molecules, the CT state generally exhibits a long decay time as compared to that of the initially excited state.[25] As stated above, the fluorescence lifetime of nanoparticles monitored at 2.48 and 2.32 eV is about 2.5 times that for the monomer. Therefore, it is likely that the charge transfer occurs in PDDP nanoparticles and the increased fluorescence lifetime originates from the CT state. The short fluorescence lifetime of nanoparticles monitored at 2.68 eV, τ'_{463}, which is near to that of monomer, indicates that the 2.68 eV emission feature of nanoparticles also originates from the same state, S_1. The double-exponential decay of nanoparticles monitored at 2.68 eV is due to the overlap between S1 and CT states. Moreover, the line shape of each nanoparticle emission spectrum in Figure 5 does not change as the excitation energy is varied between the energy determined from the same nanoparticle size absorption spectrum, E[$S_0(0)-S_1(n)$] (corresponding to excitation directly into S_1) and E[$S_0(0)-CT(n)$] (with excitation into the CT state). This indicates that, in PDDP nanoparticles, S1 and CT are in equilibrium at room temperature and the probability of the emission transition [$S_1(0)-S_0(0)$] decreased with increasing nanoparticle size.

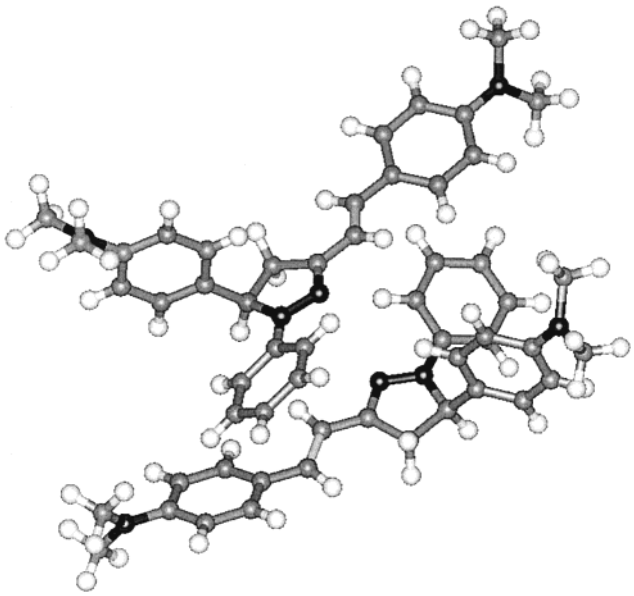

Figure 8. Optimized structures of the two-PDDP-molecule pair in nanoparticles.

Optical Size Dependence of PDDP Nanoparticles. This optical size-dependent property of PDDP nanoparticles, which appears in nanoparticles ranging from tens to hundreds nanometers, differs from the so-called "quantum confinement effect" which is observed in semiconductor fine particles whose sizes are less than 10 nm.[1] The size dependence of PDDP nanoparticles is also unlikely to be due to Mie scattering, which is often observed in metal nanocrystals. Actually, Mie scattering can affect the peak position of absorption spectra; however, the change in the peak widths of the spectra in Figure 2 cannot be explained by Mie scattering.[8] In fact, the cause for this peculiar phenomenon is not clear. To explain the same size dependence of perylene nanoparticles as that in our experimental results, Nakanishi suggested two reasons.[8,9] One is the change of lattice state due to the increase in surface area. It is likely that the increase in surface area causes lattice softening, and therefore the Coulombic interaction energies between molecules become smaller, leading to wider band gaps. The other reason may be the electric field effect of surrounding media through the surface of nanoparticles. The same ξ-potential of PDDP nanoparticles with different sizes and shapes indicates that the latter is not, at least, the principal reason for the optical size dependence of PDDP nanoparticles.

In 2-pyrazolines, the charge distribution of N-1 (N at the 1-position) changes from negative in the ground state to positive in the excited state because of the conjugated charge transfer from N-1 to C-3.[16,17] Thus, 2-pyrazolines possess a large dipole moment and hyperpolarizability. For example, the dipole moment of PDDP is about 4.34 D.[13] Considering the steric effect of the phenyl ring at the 5-position and the orientation of the dipole moment, and referring to the crystal structure of the similar 1,3-diphenyl-2-pyrazoline,[26] the optimized structure of the two-PDDP-molecule pair in a nanoparticle is proposed as shown in Figure 8. The intermolecular charge transfer may occur from N-1 of one molecule to the neighbors, leading to the decrease in the probability of optical transitions that involves the n electrons of nitrogen. This is supported by the simultaneous occurrence of the relative oscillator strength decrease of [$S_0(0)-S_2(0)$] (n−π* type) and the relative oscillator strength increase of [$S_0(0)-CT(n)$] with increasing nanoparticle size (cf.

(21) Tanaka, J. *Bull. Chem. Soc. Jpn.* **1963**, *36*, 1237.
(22) Kelly, M. K.; Etchegoin, P.; Fuchs, D.; Kratschmer, W.; Fostiropoulos, K. *Phys. Rev. B* **1992**, *46*, 4963.
(23) Bulovic, V. P.; Burrows, E.; Forrest, S. R.; Cronin, J. A.; Thompson, M. E. *Chem. Phys.* **1996**, *210*, 1−12.
(24) Pope, M.; Swenberg, C. E. *Electronic Processes in Organic Crystals*; Oxford University Press: Oxford, 1982
(25) Schulman, S. G. *Fluorescence and Phosphorescence Spectroscopy: Physicochemical Principles and Practice*; Oxford: New York, 1977.
(26) Duffin, B. *Acta Crystallogr. B* **1968**, *24*, 1256.

Figure 3). The increase in the relative oscillator strength of this CT peak with increasing the nanoparticle sizes reflects the formation process of CT states in nanoparticles. Moreover, its position was observed to shift to the low-energy side from 2.83 to 2.73 eV as the nanoparticle sizes were increased from 20 to 310 nm, and the value of energy decrease amounts to −0.1 eV. A similar red shift in the CT peak in PTCDA/InPc-Cl multilayer structures has also been observed.[27] In that case, an energy decrease of about 80 meV was obtained for an increase in PTCDA thickness from 3 to 250 Å and has been attributed to the change in the CT exciton binding energy as a result of quantum confinement in a finite potential well.[28] That is, as the nanoparticle size is decreased, the exciton overlaps with fewer molecules—the exciton radius reduces, and so the dipole moment is reduced.

From Figure 8, we can see that the phenyl and the pyrazoline rings of the two neighbor molecules overlap to some extent. As the nanoparticle size increases, the degree of these chromophores' overlap would be enhanced and would result in their absorption shifting to lower energy. In fact, the Nakanishi viewpoint is from bulk to mesoscopic. If reversed, from molecular level to mesoscopic, the occurrence of CT in nanoparticles leads to a larger increase in the dipole moment than the monomer does. As the nanoparticle size increases, CT states gradually form and the overlap of the pyrazoline rings is gradually enhanced. Therefore, the increase in the intermolecular dipole−dipole interaction leads to a narrow band gap. In addition, because of the inverse orbital orientation of n electrons of nitrogen atoms, the orbital overlap between them is small, leading to little change of the n−π* absorption with different nanoparticle sizes. The coexistence of emission transitions [$S_1(0)-S_0(0)$] and [$CT(0)-S_0(0)$] indicates that, in nanoparticles, the S1 state and the CT state are in equilibrium. The occurrence probability is different for different naoparticle sizes, which suggests that they compete with each other and are affected by the nanoparticle size.

Conclusion

In summary, we have successfully prepared PDDP nanoparticles with a series of sizes by the simple reprecipitation method. Using the absorption and fluorescence spectra of different size nanoparticles and the dilute PDDP/ethanol solution, the electronic transitions of this interesting PDDP molecular crystal have been studied. We identify Frenkel-like states which result from the individual molecules and are in the absorption spectra at $E > 3.0$ eV, and we find that the feature in the region of 2.83−2.73 eV is a charge-transfer exciton stemming from the close stacking of PDDP molecules in nanoparticles. Evolution of the CT peak with increasing nanoparticle sizes unambiguously identifies this state as being due to PDDP aggregates, and also is confirmed by the time-resolved fluorescence measurements. Moreover, the CT peak is observed shifting to the low-energy side with increasing nanoparticle size due to exciton confinement. The energy decrease of the S1 state accompanying an almost unchanging S2 state is explained by the overlap degree of the n or π orbital and the intermolecular interaction as a function of nanoparticle sizes. In nanoparticles, the S1 and CT states are in equilibrium, and the energy space between them decreases with increasing nanoparticle size. The redistribution of emission intensity from the S1 state to the CT state with increasing nanoparticle size indicates that the S1 state and the CT state compete with each other and are affected by the nanoparticle size, and this is supported by the excitation spectra.

Experimental Section

Materials. The compound 1-phenyl-3-((dimethylamino)styryl)-5-((dimethylamino)phenyl)-2-pyrazoline (PDDP) was synthesized according to ref11 and confirmed by NMR and MS. PDDP nanoparticles

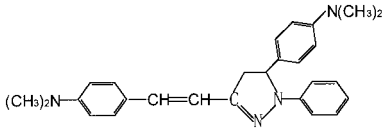

PDDP

were prepared as follows: quantities of a PDDP/ethanol solution (1.0×10^{-3} mol·L^{-1}) were injected into 10 mL of water with vigorous stirring, using a 100 μL microsyringe. PDDP molecules began to aggregate at once, and a dispersion of its nanoparticles in water was obtained. By controlling the quantity of PDDP/ethanol solution injected into water and the temperature, the size of the nanoparticles was controlled. For example, when 40 and 100 μL amounts of the PDDP/ethanol solution were injected, the nanoparticle sizes finally prepared were 50 and 105 nm at 25 °C or 90 and 190 nm at 50 °C, respectively.

Methods. The UV−visible absorption spectra of nanoparticles dispersions in water were measured using a Shimadzu UV-1601 PC double-beam spectrophotometer. The steady-state excitation and emission fluorescence spectra were recorded with a Hitachi F-4500 spectrometer. Time-resolved fluorescence measurements were carried out by using a time-correlated single-photon counting (TCSPC) method. A cavity-dumped dye laser (M3500, SP) synchronously pumped by a mode-locked YAG laser (M3800, SP) was employed as an excitation source. The dye laser was operated using Rh 6G dye with a tuning range of 290−320 nm, and the laser pulse which has an 800 kHz repetition rate and <100 ps pulse width was doubled using a 390 frequency doubler (SP) to excite the sample. Fluorescence was selected into a double monochromator with an MCP-PMT (E3059-00, Hamamatsu) for detection. All of the standard electronics used for TCSPC were EG&G Ortec, except for the Tennelec 454 constant fraction discriminator. The maximum count was 10 000.

The sizes and shapes of the nanoparticles were observed by means of field emission scanning electron microscopes (FESEM, Amray 1910FE and JSM-6301F). The sizes and distributions of nanoparticles dispersed in water were also evaluated by dynamic light scattering (DLS) using a Zetaplus BI-9000 (Brookhaven Instruments Corp., Holtsville, NY). The same instrument measured the surface electric ξ-potential of nanoparticles.

Molecular modeling calculations were carried out using CHEM3D Pro 4.0, which was developed by CambridgeSoft Corp., Cambridge, MA. Molecular modeling was done on a Pentium 266 using a MM2 force field. The structure of the two-PDDP-molecule pair in nanoparticles was drawn, and the minimum energy configuration was obtained by energy minimization under a vacuum. The modeling was also done using the PM3 semiempirical quantum mechanical method for the two-PDDP-molecule pair in a nanoparticle. The minimization procedure involves systematically altering the coordinates of the atoms and estimating the conformation until a minimum energy configuration was reached.

Acknowledgment. This paper was sponsored by the National Natural Foundation of China. The support of this research by the National Research Fund for Fundamental Key Projects No.973 (G19990330) and the Chinese Academy of Sciences is also gratefully acknowledged.

JA0026298

(27) Anderson, M. L.; Williams, V. S.; Schuerlein, T. J.; Collins, G. E.; England, C. D.; Chau, L.-K.; Lee, P. A.; Nebesny, K. W.; Armstrong, N. R. *Surf. Sci.* **1994**, *307−309*, 551.

(28) Forrest, S. R. *Chem. Rev.* **1997**, *97*, 1793−1896.